Smad5 knockout mice die at mid-gestation due to multiple embryonic and extraembryonic defects

Hua Chang[1,4], Danny Huylebroeck[5], Kristin Verschueren[5], Qiuxia Guo[1], Martin M. Matzuk[1,2,3,4,*] and An Zwijsen[5]

Departments of [1]Pathology, [2]Cell Biology and [3]Molecular and Human Genetics, and [4]Program in Developmental Biology, Baylor College of Medicine, Houston, TX, 77030, USA
[5]Department of Cell Growth, Differentiation and Development (VIB07), Flanders Interuniversity Institute for Biotechnology (VIB) and Laboratory of Molecular Biology, University of Leuven, Belgium
*Author for correspondence (e-mail: mmatzuk@bcm.tmc.edu)

SUMMARY

Smad5 has been implicated as a downstream signal mediator for several bone morphogenetic proteins (BMPs). To understand the in vivo function of Smad5, we generated mice deficient in Smad5 using embryonic stem (ES) cell technology. Homozygous mutant embryos die between E9.5 and E11.5, and display variable phenotypes. Morphological defects are first detected at E8.0 in the developing amnion, gut and heart (the latter defect being similar to BMP-2 knockout mice). At later stages, mutant embryos fail to undergo proper turning, have craniofacial and neural tube abnormalities, and are edematous. In addition, several extraembryonic lesions are observed. After E9.0, the yolk sacs of the mutants contain red blood cells but lack a well-organized vasculature, which is reminiscent of BMP-4, TGF-β1 and TGF-β type II receptor knockout mice. In addition, the allantois of many *Smad5* mutants is fused to the chorion, but is not well-elongated. A unique feature of the *Smad5* mutant embryos is that ectopic vasculogenesis and hematopoiesis is observed in the amnion, likely due to mislocation of allantois tissue. Despite the expression of *Smad5* from gastrulation onwards, and in contrast to knockouts of Smad2 and Smad4, Smad5 only becomes essential later in extraembryonic and embryonic development.

Key words: BMP, TGF-β, Amnion, Yolk sac, Vasculogenesis, Hematopoiesis, Mouse

INTRODUCTION

Growth factors of the TGF-β family signal via heteromerization of type II and type I serine/threonine kinase receptors (reviewed by Massagué and Weis-Garcia, 1996). Upon ligand binding to the type II receptor, the constitutive kinase of the type II receptor activates the type I receptor by phosphorylation, which, in turn, activates the downstream signal transduction cascade. Recent studies have shown that Smad proteins, first identified through genetic screens in *Drosophila* and *Caenorhabditis elegans*, play pivotal roles in transducing signals from TGF-β ligands (reviewed by Attisano and Wrana, 1998). At least nine different mammalian Smad proteins have now been identified and they are classified into three subgroups based on their functions. In response to ligand-induced activation of type I receptors, receptor-regulated Smads become phosphorylated and translocate to the nucleus. Biochemical studies have shown that Smad1, Smad5 and Smad8 transduce signals for BMPs, while Smad2 and Smad3 appear to be specific for signaling of TGF-βs and activins. As a common component of different pathways, Smad4 oligomerizes with activated Smads and the complex translocates to the nucleus where gene regulation can take place. Smad6 and Smad7 function as antagonists in the signaling process by forming a stable interaction with type I receptors and blocking the activation of receptor-regulated Smads (reviewed by Attisano and Wrana, 1998; Heldin et al., 1997).

Smad5 is highly homologous to Smad1 and was suggested to be a component of the BMP pathway. Ectopic expression of Smad5 in the amphibian embryo induces ventral mesoderm similar to BMP-2, BMP-4 or Smad1 (K. V., C. Niehrs and D. H., unpublished results; Meersseman et al., 1997; Suzuki et al., 1997). In vitro studies have also demonstrated that Smad5 is directly activated by BMP type IA (ALK-3) or type IB (ALK-6) receptors, and a dominant negative variant of Smad5 can specifically inhibit downstream gene expression induced by BMP-2 and BMP-4 (Yamamoto et al., 1997; Nishimura et al., 1998). Smad5 has also been implicated in BMP-7 signal transduction (Macias-Silva et al., 1998; Tamaki et al., 1998). Recently, antisense technology showed that the inhibitory effect of TGF-β on hematopoietic cell proliferation is mediated through Smad5, possibly extending the array of action of Smad5 towards TGF-β signal transduction (Bruno et al., 1998). Northern blot analysis and in situ hybridization (Meersseman et al., 1997) showed that *Smad5* is present throughout

postimplantation mouse development and in many adult tissues.

Gene knockouts of several TGF-β family members, their receptors or downstream signaling proteins have demonstrated the essential role of these proteins in mouse embryogenesis (reviewed by Lau et al., 1997). *Smad4* mutant embryos fail to initiate gastrulation and die before E7.5 (Sirard et al., 1998; Yang et al., 1998). The lack of mesoderm formation and retarded growth observed in *Smad4* mutant embryos is similar to the phenotype observed in some of the *BMP-4* mutant embryos (Winnier et al., 1995) and all *ALK-3* mutants (Mishina et al., 1995); however, abnormal visceral endoderm development is also observed in the Smad4 null embryos. Since Smad4 is a common component in multiple signal transduction pathways of the TGF-β family, it is not surprising that Smad4-deficient mice have a more severe phenotype compared to any single ligand or receptor knockout mouse reported thus far. Likewise, *Smad2* knockout embryos die early in embryogenesis due to defective mesoderm formation (Nomura and Li, 1998; Waldrip et al., 1998; Weinstein et al., 1998), a more severe phenotype than the phenotypes observed in knockouts of its putative upstream activating ligands (i.e., activins and TGF-βs); however, resemblance to nodal-deficient embryos (Conlon et al., 1994) is striking in that extraembryonic ectoderm proliferates into the epiblast (Nomura and Li, 1998; Weinstein et al., 1998). Although both Smad2 and Smad3 have been implicated in the signaling of TGF-βs and activins, *Smad3* knockout mice are viable and develop metastatic colorectal cancer (Zhu et al., 1998).

Little is known about the in vivo function of Smad5 in mouse embryogenesis. To understand its physiologic function and its relationship with upstream activators, we have generated a loss-of-function mutation of Smad5 in mice using ES cell technology. Our data demonstrate an essential role of Smad5 at mid-gestation and provide important clues of the in vivo relationships between Smad5 and TGF-β superfamily ligands and receptors.

MATERIALS AND METHODS

Construction of the Smad5 targeting vector and generation of mice carrying the *smad5*[m1] allele

A mouse 129SvEv genomic library was screened with a 2.3 kb mouse *Smad5* cDNA probe (Meersseman et al., 1997), and the seven exons of *Smad5* were mapped and sequenced (unpublished results). The Smad5 targeting vector included PGK-*hprt* and MC1-*tk* expression cassettes (Matzuk et al., 1992) for positive and negative selection, respectively. The targeting vector contained 2.1 kb of homology on the 5′ arm and 6.1 kb of homology on the 3′ arm. The linearized *Smad5* targeting vector was electroporated into AB2.1 ES cells (129SvEv). Electroporated cells were cultured in the presence of HAT (hypoxanthine, aminopterine and thymidine) and FIAU 1-(2′-deoxy-2′-fluoro-β-D-arabinofuranosyl)-5′-iodouracil as described (Matzuk et al., 1992). Correctly targeted ES cell clones were expanded and three independent ES cell lines were injected into C57Bl/6 blastocysts to obtain chimeric mice (Bradley, 1987) to produce C57Bl/6/129SvEv hybrid F₁ progeny. The majority of the results were obtained from mice derived from ES cell line Smad5-80-D11.

Genotype analysis

Southern blot analysis was performed using the 3′ external probe to genotype tail DNA and yolk sac DNA isolated from mice older than

E10.5 (Fig. 1B). E8.5 and E9.5 embryos were genotyped by PCR analysis of yolk sac DNA (Fig. 1C). One set of primers was derived from the human *hprt* minigene and the flanking *Smad5* genomic region (5′ sequence: 5′-GAGACTAGTGAGACGTGCTACTTCC-3′, 3′ sequence: 5′-CATGCAAATTGGGGAGGTACACGTT-3′) and a second set of primers derived from the deleted region and the flanking region (5′ sequence: 5′-TCTGGCCTCTTAATCCTGGACTTTCC-3′, 3′ sequence: 5′-TAAGAGAGTGGAGAGTCCAGGTAAG-3′). The PCRs were performed as follows: 94°C, 3 minutes followed by 30 cycles of: 94°C for 30 seconds, 60°C for 1 minute, 72°C for 1 minute and then one cycle at 72°C for 7 minutes. A 500 bp fragment derived from the mutant allele and a 700 bp fragment derived from the wild-type allele were resolved on 1.3% agarose gels. Embryos younger than E8.5 were analyzed by in situ hybridization on tissue sections with the Smad5 probe to determine whether they were *Smad5*-negative or *Smad5*-positive.

Histological analysis

Embryos were dissected from the uterus and fixed in 4% (w/v) paraformaldehyde at 4°C overnight. After dehydration in an increasing ethanol series, embryos were embedded in paraffin, sectioned (5 or 6 μm), and stained with hematoxylin and eosin.

In situ hybridization

Whole-mount in situ hybridization was performed as described (Albrecht et al., 1997). Embedding of decidua and embryos and radioactive in situ hybridization on paraffin sections was performed as described previously (Dewulf et al., 1995). The antisense RNA probes used were *AP-2* (Zhang et al., 1996), *flk-1* (C. De Vries, Amsterdam, personal gift), *GATA-4* (Molkentin et al., 1997), *HNF3β* (Ang et al., 1993), *Nkx*2.5 (Lints et al., 1993), the proline-rich domain of *Smad5* (Meersseman et al. 1997), *twist* (Chen and Behringer, 1995) *ζ-globin* (Leder et al., 1992) and *Tbx2* (R. Schwartz, Houston, personal gift).

RESULTS

Targeted disruption of the mouse *Smad5* gene and generation of *Smad5* knockout mice

The mouse *Smad5* gene contains seven exons with the protein coding sequence initiating in the middle of exon 2. We designed a gene targeting construct to replace exon 2 and flanking sequences (1.5 kb in total) with a PGK-*hprt* expression cassette inserted in the opposite orientation (Fig. 1A). A transcriptional terminator sequence was also introduced into intron 1. Since exon 2 contains the translation initiation codon and encodes about one third of the whole protein (134 amino acids) and none of the downstream ATGs are in an appropriate Kozak sequence, deletion of exon 2 was predicted to generate a null allele. 59% of the ES clones were correctly targeted (71 out of 120 clones screened) and male chimeras, derived from three ES cell lines, transmitted the mutant allele to progeny (Fig. 1B). *Smad5* mutant heterozygotes (*smad5*[m1]/+) were phenotypically normal and crossed to generate *Smad5* homozygous mutant (*smad5*[m1]/*smad5*[m1]) mice.

Loss of Smad5 results in embryonic lethality

Although *smad5*[m1]/+ mice were fertile and normal, we failed to detect any liveborn homozygous offspring from heterozygote breedings (Fig. 1B; Table 1) indicating that *Smad5* homozygous mutant mice died during embryogenesis. Timed matings of *smad5*[m1]/+ mice were initiated to obtain

embryos at different developmental stages. A normal 1:2:1 Mendelian ratio was evident up to E10.5 litters (Fig. 1C; Table 1). *Smad5* homozygous mutant embryos could be recovered but died between E9.5 and E11.5 (Table 1) with a variable phenotype even within a litter (Fig. 2; Table 2). All mutant embryos proceeded beyond the egg cylinder stage, underwent gastrulation and initiated organogenesis. The mutant phenotype was first evident at E8.0-E8.5 when some embryos (6/11) were noted to have vestigial foregut and hindgut (Fig. 2B,D; Table 2) and/or abnormal amnion morphology. In some of the mutants, the heart was not enclosed by the body wall and remained exteriorized. Additionally, the posterior region of the embryo extended proximally far above the level of the head folds, which was probably a result of the altered (more anterior) body curvature and/or the poorly elongated allantois (Fig. 2D,H). Furthermore, the allantois had an enlarged base (Fig. 2D). In mutants with milder phenotypes, gut and heart development seemed to be almost normal, but an aggregate of cells was often noted on the amnion (Fig. 2D).

At E9.5, *Smad5* mutant embryos had developed several anomalous features with variable degrees of severity. Defects suggesting impaired vasculogenesis and hematopoiesis were observed in both mildly and severely affected *Smad5* mutants. The yolk sac of the mutants lacked distinctive networks of branching vitelline vessels and appeared anemic (Fig. 2E-G). The embryonic vasculature also appeared to be affected since many embryos were edemic (Fig. 2J,K). Hemorrhagic structures were often seen on the amnion of the mutant embryos (Fig. 2G,J,K,M). In addition, all mutant embryos had defects in turning at E9.5. In the most severely affected embryos, a general developmental delay was observed, embryos were reduced in size, the heart was exteriorized and underdeveloped, turning was never initiated (Fig. 2H), and the midgut and hindgut remained open (Fig. 2J,M). In some embryos, failure of cranial neural tube closure resulted in exencephaly, the development of the prosencephalon and optic sulcus was delayed (Fig. 2D,J), and the branchial arches were underdeveloped (Fig. 2J,K). In contrast to the *BMP-4* knockout embryos (Winnier et al., 1995), somitogenesis was largely unaffected by the absence of Smad5. Although several embryos recovered at E9.5 had started to disintegrate, some advanced mutant embryos with up to 36 somites were still alive at E10.5 (Fig. 2M-O). In these embryos, anterior structures were relatively less affected, forelimb and hindlimb buds were developed, but the posterior region was fragile and poorly organized. Heart development was severely delayed compared to brain and somite development,

Table 1. Genotype of progeny from *smad5*[m1] heterozygous crosses

Stage	+/+	+/−	−/− (%)	Total
E8.5	15	27	12 (22%)	54
E9.5	13	26	15 (27%)	54
E10.5	6	12	7 (28%)	25
E11.5	6	13	4 (17%)	23
E12.5	5	11	1 (6%)	17
E13.5	4	10	0 (0%)	14
Weaning	152	252	0 (0%)	404
	(37.6%)	(62.4%)		

The Mendelian ratio 1:2:1 was observed for embryos collected from E8.5 to E10.5. From E11.5 onwards, fewer homozygous (−/−) mutants were represented. Although the number of heterozygotes (+/−) is less than twice that of the wild-type (+/+) siblings in mice at weaning, there is no significant deviation from the Mendelian ratio as estimated by χ^2 analysis.
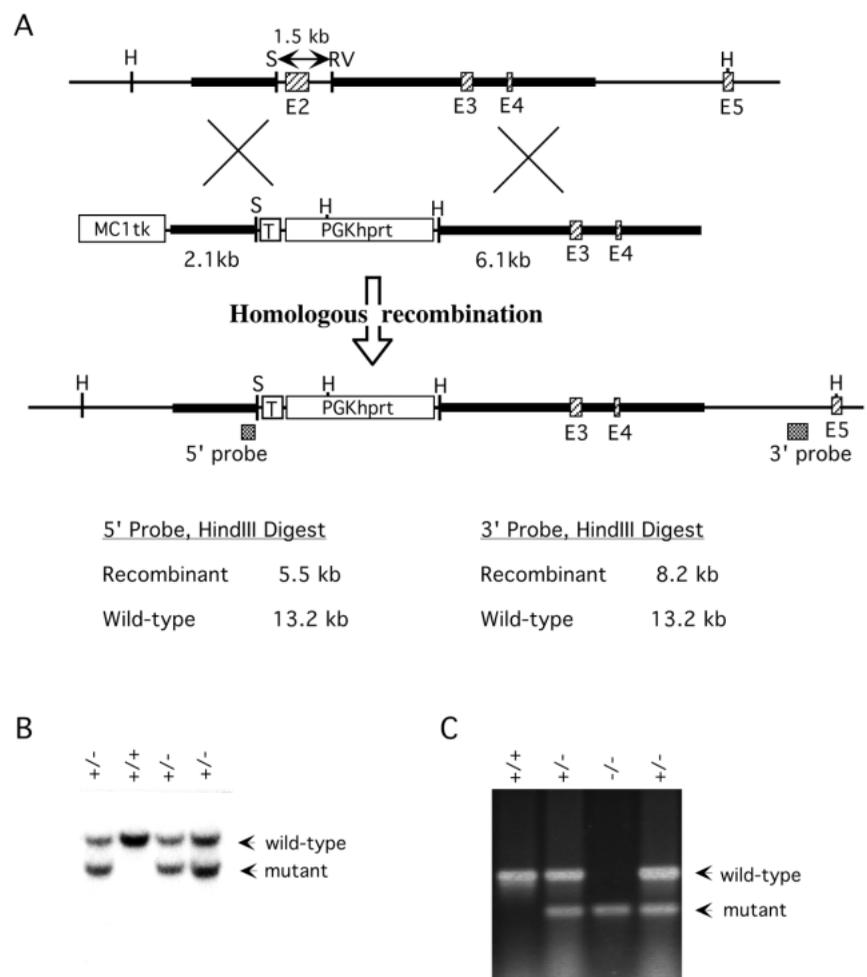

Fig. 1. Targeting of the *Smad5* gene in ES cells and genotype analysis of offspring from heterozygote intercrosses. (A) Smad5 wild-type locus, the targeting vector and the *smad5*[m1] mutant allele (top to bottom). The targeting vector deletes exon 2 and flanking region. PGK-*hprt* and MC1-*tk* expression cassettes are shown. T indicates bovine growth hormone transcriptional terminator sequence. Recombinants were detected by Southern blot analysis using 5′ and 3′ probes and *Hin*dIII (H) as the diagnostic enzyme. RV, *Eco*RV; S, *Spe*I. (B) Southern blot analysis of genomic DNA isolated from mice at weaning generated from intercrosses of *smad5*[m1]/+ mice. No liveborn homozygous mutants were recovered. +/+, wild-type; +/−, heterozygote. (C) PCR genotype analysis of yolk sac DNA collected from *Smad5* heterozygote timed matings. Homozygotes (−/−) could be recovered at a normal Mendelian ratio at E8.5 and E9.5.

Fig. 2. Morphologic appearance of *smad5*[m1]/*smad5*[m1] and wild-type embryos at several stages of development. Frontal view of (A) a wild-type (WT) and (B) a *smad5*[m1]/*smad5*[m1] (–/–) embryo, demonstrating a delay in foregut invagination in the mutant. The cross-like structure is the headfold which is evident through the yolk sac due to the lack of a foregut pocket. Lateral view of (C) E8.5 wild-type and (D) mutant embryos dissected free from yolk sac. Both embryos have 8 pairs of somites. Note the enlarged base of the allantois in D (asterisk). The mutant embryo has an extreme anterior body curvature (arrowhead). (E) E9.5 control and (F,G) homozygous mutant conceptuses within the yolk sac. Control yolk sacs have a well-developed vascular network containing red blood cells. Mutant yolk sacs are devoid of a blood-filled network of vessels, but still develop a primitive plexus. Transverse sections at the level of a and b in F are shown in Figs 4E and 6E, respectively. (G,J,M) A hemorrhagic aggregate of blood cells is present on the amnion. (H) The embryo (E9.5) has a severe phenotype. Although the mutant developed up to 11 pairs of somites, it did not initiate turning. Furthermore, the heart is exteriorized and the body curvature is extremely anterior (arrowhead). The anterior and posterior ends of the embryo are closely apposed. (I) An E9.5 control and (J,K) a less severely affected, turned mutant embryo. Craniofacial structures and brain development are impaired and the gut remains open. (L) E10.5 control and (M-O) mutant embryos. Embryonic turning was not complete since the tip of the tail directed to the lefthand side.
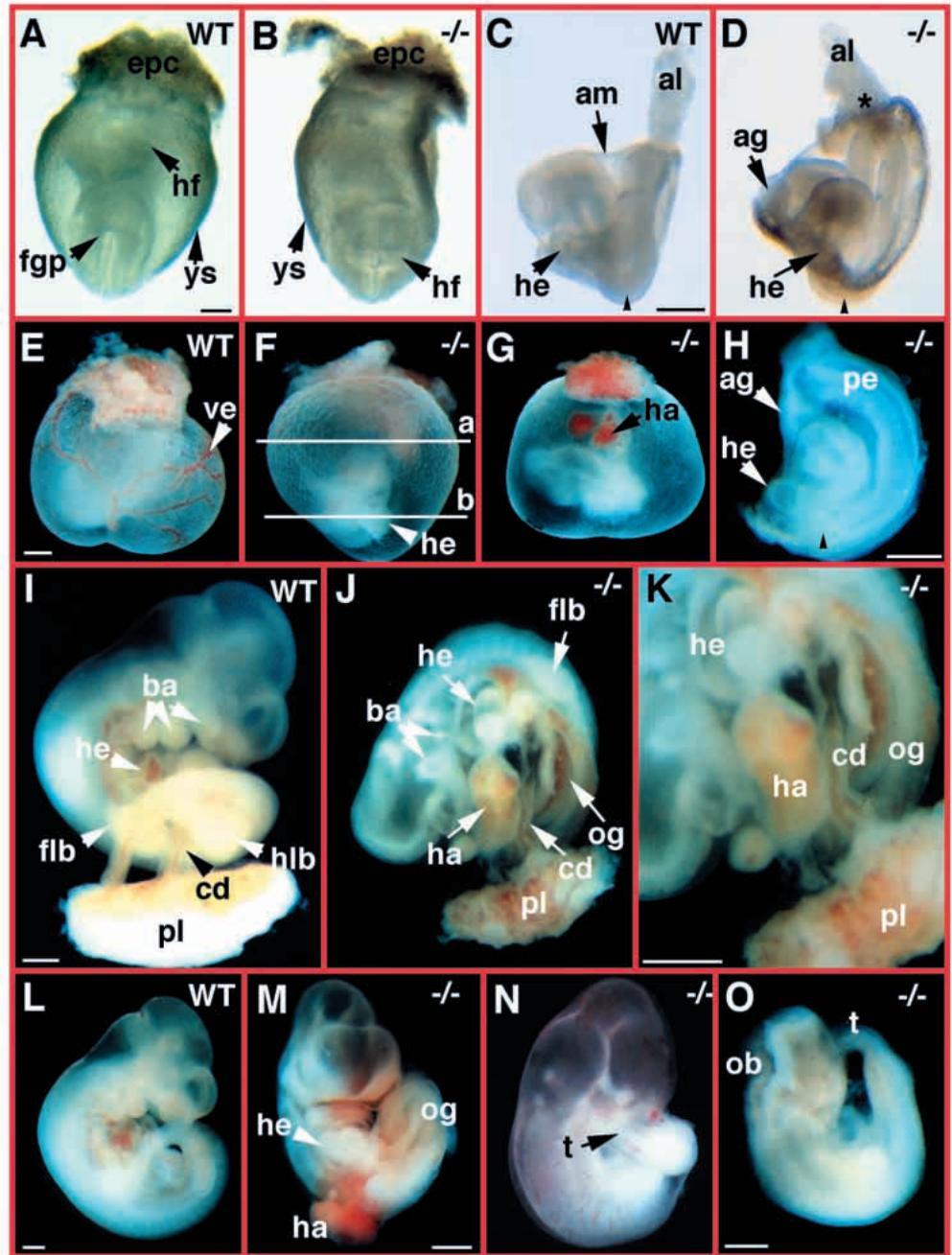
Abbreviations: ag, aggregate of cells; al, allantois; am, amnion; ba, branchial arches; cd, umbilical cord; epc, ectoplacental cone; fgp, foregut pocket; flb, forelimb bud; ha, hemorrhagic aggregate of cells; he, heart; hf, headfold; hlb, hindlimb bud; og, open midgut; ob, open mid-hindbrain; pe, posterior end; pl, placenta; t, tail; ve, vitelline vessels; ys, yolk sac. Scale bar: (A-D) 200 μm; (E-O) 500 μm.

Table 2. Prevalence of defects in *Smad5* mutant embryos

Embryonic age	Amnion-allantois defects*	Heart in exocoelomic cavity‡	Gut defects	Turning defects§	Yolk sac vasculogenesis defects	Branchial arch defects	Neural tube defects
E8.5	18/19	ND¶	6/11	13/15	NA	NA	NA
E9.5	10/11	5/11	11/11	11/11	11/11	7/11	3/11
E10.5	5/6	2/6	6/6	6/6	6/6	6/6	2/6

*Amnion-allantois defects included the appearance of an aggregate of cells on the amnion and a poorly elongated allantois with an enlarged base.

‡Delayed heart development compared to the overall development of the embryo was not included.

§Turning defects included failure to initiate turning in embryos with more than 10 pairs of somites, failure to complete turning in embryos with more than 18 pairs of somites, and tail pointing in the opposite direction.

¶ND, not determined; NA, not applicable.

the posterior body wall remained open, and turning was not properly completed or was in the opposite direction (Fig. 2M-O). All *Smad5* mutant embryos died by E11.5 and were resorbed after E12.5. The above-mentioned defects in extraembryonic and embryonic development in *Smad5* knockout embryos will be described in more detail in the following sections.

Expression of *Smad5* in early mouse embryos

We have reported on the expression of *Smad5* in mid-gestation mouse embryos (Meersseman et al., 1997). To further understand the observed embryonic and extraembryonic defects in our Smad5 knockout, we documented the spatial expression pattern of *Smad5* earlier in embryonic development by in situ hybridization. In early postimplantation embryos (E6.5), *Smad5* was detected uniformly in the epiblast, whereas the signal in extraembryonic endoderm and extraembryonic ectoderm was not above background (Fig. 3A). At E7.5, high levels of *Smad5* transcripts were detected homogeneously throughout all three embryonic germlayers (Fig. 3B). At E8.5, the extraembryonic mesoderm cells of the allantois expressed *Smad5* at a level similar to that in the embryonic cells, but the extraembryonic mesoderm of yolk sac and amnion expressed *Smad5* at a lower level, with the exception of the blood islands, which might reflect differences in tissue thickness (Fig. 3C). At E8.5 and E9.5, overall expression of *Smad5* was abundant, without significant differences in expression levels between various tissues, although the endocardium and myocardium of the heart expressed slightly lower levels of *Smad5* mRNA (Fig. 3D).

Defects in the development of extraembryonic tissues in *Smad5* mutant embryos

The most posterior mesoderm exiting the primitive streak during gastrulation, the extraembryonic mesoderm, migrates proximally and laterally into the extraembryonic region, displacing the extraembryonic ectoderm toward the ectoplacental cone (Tam and Beddington, 1992). The formation of the amnion/chorion initiates at E7.0 by the protrusion of the amniotic folds and ends with the closure of the proamniotic canal at E7.5 which then divides the proamniotic cavity into the amniotic, the exocoelomic and the ectoplacental cavities (Kaufman, 1992). The allantois is an extraembryonic mesodermal tissue that elongates from the very posterior end of the primitive streak into the exocoelomic cavity. The extraembryonic mesoderm and extraembryonic endoderm wall of the exocoelomic chamber will expand to form the yolk sac.

In *Smad5* mutant embryos, defects in the development of the amnion and allantois were observed (Fig. 4A). The allantois is always fused to the chorion to complete the chorioallantoic placental circulation, but was often poorly elongated and had an enlarged base (Fig. 4A). In most embryos, the amnion appeared not well expanded, as revealed by the close opposition of anterior and posterior regions (Fig. 4A-C). Strikingly, the surface of the amnion was not smooth, and characteristic aggregates of cells were attached to the amnion and distinguished mutants from their wild-type or heterozygous littermates (Figs 2D, 4A). These aggregates of cells were often localized next to the headfold or the heart and sometimes close to the allantois. This abnormal aggregate
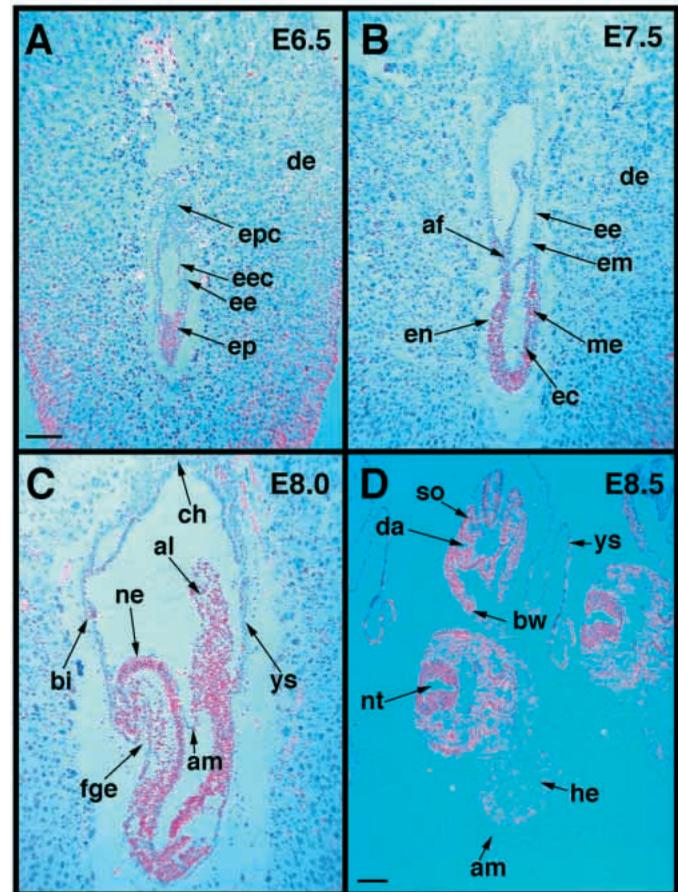

Fig. 3. Expression of *Smad5* in early postimplantation embryos analyzed by in situ hybridization. Sagittal sections through embryos of (A) E6.5, (B) E7.5 and (C) E8.0 embryos. (D) Transverse section through an E8.5 embryo. *Smad5* is expressed more abundantly in the embryo proper than in maternal tissue. Dark-field and bright-field images are superimposed, resulting in a pink hybridization signal. Anterior is to the left. Abbreviations: af, amniotic fold; al, allantois; am, amnion; bi, blood island; bw, body wall; ch, chorion; de, deciduum; da, dorsal aorta; epc, ectoplacental cone; ec, ectoderm; en, endoderm, ep, epiblast; eec, extraembryonic ectoderm; ee, extraembryonic endoderm; em, extraembryonic mesoderm; fge, foregut entrance; he, heart; me, mesoderm; ne, neuroectoderm; nt, neural tube; so, somite; ys, yolk sac. Scale bar: (A-C) 100 μm; (D) 200 μm.

of cells appeared to be derived from extraembryonic mesoderm, since the ectodermal component of the amnion was not altered in these embryos, as demonstrated by the normal in situ hybridization pattern for the transcription factor *AP-2*, a marker for non-neural surface ectoderm (Mitchell et al., 1991; Fig. 4B). However, *twist* and *Tbx2* expression were very high in the cell aggregates (Fig. 4C,D); *twist* is a basic helix-loop-helix (bHLH) transcription factor normally expressed in the extraembryonic mesoderm of the amnion and allantois at this stage (Stoetzel et al., 1995); *Tbx2* is a member of the T-box-containing transcription factors (reviewed by Papaioannou, 1997) expressed strongly in myocardiogenic progenitor cells and allantois, but not noticeably in the amnion. These data suggest that the aggregate of cells observed on the mutant amnion are likely

due to mislocation of allantois tissue. Vasculogenesis and hematopoiesis in the aggregate of cells on the amnion was revealed at E8.5 by *flk-1* and *ζ-globin* in situ hybridization (Fig. 4F,G). *Flk-1* encodes a receptor for vascular endothelial cell growth factor (VEGF) and is an early marker for blood islands and endothelium (Millauer et al., 1993). Embryonic *ζ-globin* is a marker for primitive red blood cells (Leder et al., 1992). Histological analysis of the hemorrhagic structure in E9.5 mutants demonstrated the presence of a wide variety of cell types including endothelial cells organized into distinct vessels filled with blood (Fig. 4E) resembling allantois tissue.

The onset of vasculogenesis and hematopoiesis in the mouse is defined by the appearance of discrete blood islands in the yolk sac at approximately E7.5-E8.0. Hemangioblasts arise from extraembryonic mesoderm-derived precursors and differentiate to hematopoietic and endothelial cells, which will form a primitive vascular plexus. Subsequently, the emerging vascular plexus is rapidly remodeled to assemble into a network with larger vitelline vessels and smaller capillaries. Histological and morphological examination of yolk sacs at E8.5 showed no obvious morphological defects in *smad5*[m1]/*smad5*[m1] embryos compared to control littermates. All yolk sacs were of similar size, well-expanded and possessed corona, characteristic of developing blood islands. However, a number of yolk sacs of late E8.5 mutants seemed to already contain larger numbers of primitive blood cells (Fig. 4K,M) whereas a few contained almost none at E9.5 (data not shown). By E9.5, all of the mutant yolk sacs appeared morphologically anemic and had disorganized and fragile vessels or lacked vitelline vessels (Fig. 2F,G), yet possessed a primitive plexus, indicative of the onset of normal vasculogenesis. Histological analysis demonstrated that the extraembryonic endoderm and mesoderm layers of the yolk sac were often only loosely attached to each other, a finding never observed in controls after fixation (Fig. 4H,I). Likewise, the integrity of the vessels in the embryo proper was also affected. The dorsal aortae and vitelline vessels were much more dilated in the mutants compared to controls although they still contained red blood cells (Fig. 4F,G,K,M).

To further understand the defects in vascular development, we analyzed *flk-1* and *ζ-globin* expression by in situ hybridization. At E8.5, *flk-1* transcripts were detected in the developing vascular network, including extraembryonic yolk sac mesoderm, dorsal aorta, endocardial and intersegmental vessels, both in the wild-type and *Smad5* mutant embryos (Fig. 4J-K). Similarly, *ζ-globin*-positive cells were ubiquitous in wild-type and *smad5*[m1]/*smad5*[m1] blood islands in the yolk sac, and in heart and aorta in the embryo proper (Fig. 4L,M). These data demonstrate a normal onset of vasculogenesis and hematopoiesis in *Smad5* mutant embryos. However, the expression pattern of *flk-1* and *ζ-globin* is not completely normal. First, in some mutant embryos, increased *flk-1* and *ζ-globin* expression was detected in the extraembryonic mesoderm of the yolk sac when compared to littermate controls. Second, ectopic *flk-1* and *ζ-globin* expression was observed in the mutant amnion, much higher in the aggregates of cells, suggesting that these cells are the precursor cells of the hemorrhagic structures seen at later stages (Fig. 2G,J,K,M). The initial observation of yolk sac anemia at E9.5 was likely due to the leakage of primitive blood cells into the exocoelomic cavity (Fig. 4K,M) and poor apposition of extraembryonic endoderm with mesoderm (Fig. 4H,I) in many mutant embryos.

Gut defects in *Smad5* mutant embryos

Definitive endoderm gives rise to the lining of the gut. Fate mapping studies have provided evidence for a gradual transition from primitive to definitive endoderm during gastrulation (Lawson and Pederson, 1987; Tam and Beddington, 1992), although chimeric experiments show that the most anterior foregut and posterior hindgut endoderm still contain descendants of the primitive endoderm lineage (Rhinn et al., 1998; Narita et al., 1997; Zwijsen et al., 1999). The definitive endoderm is established by the recruitment of ectodermal cells via direct insertion or migration through the node and most anterior part of the primitive streak (Kaufman, 1992).

An obvious defect in the *smad5*[m1]/*smad5*[m1] embryos was the lack of both a foregut pocket and the entrance of the hindgut diverticulum in late headfold-to-early-somite-stage embryos (E8.0) (Fig. 2A,B). Although the initial absence of a foregut and hindgut pocket was no longer evident at later stages of development, the foregut often had a flattened and asymmetrical appearance (Fig. 4K) and the lateral body wall rarely closed around the ventral midgut region (Fig. 2J,K,M). An asymmetrical gut is often observed when notochord differentiation is affected [e.g., in the *Brachyury T* knockout (Beddington et al., 1992) and *HNF3β* knockout (Ang and Rossant, 1994)] mice. To further investigate gut abnormalities in the mutant embryos, we decided to analyze the expression pattern of *HNF3β*, a marker for endoderm, notochord and floor plate (Ang et al., 1993), prior to and just after the morphological abnormalities became apparent. At the late streak stage (E7.5), *HNF3β* expression was found in the node, in anteriorly migrating mesoderm and endoderm cells of the head process and the visceral endoderm. At E8.5, strong expression was observed in the notochord, foregut, hindgut, in several areas of the developing brain and neural tube. No aberrant *HNF3β* expression pattern was observed in the *smad5*[m1]/*smad5*[m1] embryos at E7.5, late E8.5 or E9.5 (Fig. 5), indicating that the differentiation towards and maintenance of definitive endoderm per se was not affected by the absence of Smad5.

Cardiac and embryonic turning defects in *Smad5* mutant embryos

Smad5 deficiency was observed to often cause an aberrant localization of the heart. In the most severely affected mutants, the heart was exposed in the exocoelomic cavity (Figs 2H, 5F, 6E), a phenotype reminiscent of *BMP-2* knockout mice (Zhang and Bradley, 1996). Compared to control siblings, development of the heart was delayed in the majority of *Smad5* mutant embryos (Fig. 6A-C). For example, the two heart primordia were still not amalgamated in a number of mutant embryos with up to 11 pairs of somites (Fig. 6B), a process that normally happens when the embryo has 5-6 pairs of somites (Kaufman, 1992).

To further investigate the heart phenotype that was observed in *Smad5*-deficient embryos, we performed in situ hybridization using *Nkx2.5* and *GATA-4* as probes. It has previously been shown that application of BMP-2-soaked

beads in vivo induces ectopic expression of these cardiac-specific transcription factors (Andree et al., 1998), suggesting that BMP-2 is an upstream ligand for induction of these genes. Furthermore, the phenotypes of *GATA-4* and *Nkx2.5* knockout mice resemble the *Smad5* mutant phenotype in which there is defective formation of an organized foregut and aberrant cardiac structures due to impaired lateral-to-ventral folding (Kuo et al., 1997; Molkentin et al., 1997; Schott et al., 1998). During early mouse development, *GATA-4* is expressed in the extraembryonic endoderm, the allantois, and the cardiogenic splanchnic mesoderm and associated endoderm (Heikinheino et al., 1994). *Nkx2.5* transcripts are first detected at the early headfold stages in myocardiogenic progenitor cells and their myogenic descendants (Lints et al., 1993). If BMP-2 is essential for the normal expression of these cardiac-specific transcription factors and Smad5 plays a critical role in this induction process, we would expect altered expression patterns of these genes in the mutants.

Nkx2.5 transcripts were detected by whole-mount in situ hybridization (Fig. 6A-C) in the mutant hearts in the myocardiogenic progenitor cells and their myogenic descendants similar to control embryos (data not shown). *GATA-4* mRNA was properly expressed in the cardiogenic mesoderm and underlying endoderm (Fig. 6F,G). These data indicate that Smad5 is not essential for the expression of these cardiac-specific marker genes in vivo.

In most of the *smad5*[m1]/*smad5*[m1] embryos, axial rotation was not completed properly or had not initiated at all. Embryos that did not initiate turning when they had developed up to 11-18 pairs of somites had a remarkably close head-to-tail apposition and an extreme anterior body curvature (Fig. 2H). Embryonic turning**,** the simultaneous leftward movement of the head and tail, is normally initiated when the embryo has 6-8 pairs of somites and is completed when the embryo has 14-16 pairs of somites. As a result, the germlayers are inverted and the embryo acquires its typical fetal shape and becomes completely surrounded by extraembryonic membranes (Kaufman, 1992). The failure to turn in the *Smad5* mutants could be secondary to the physical obstruction caused by an insufficiently expanded amnion or elongated allantois and/or the altered shape of the embryo from the early-somite stage onwards. However, in the mutants where turning did occur, it was always incomplete and the caudal part of the tail often twisted in front of the head in the opposite (lefthand) direction (Fig. 2N,O; Table 2). The heart-looping and axial-rotation defects can reflect a general left/right asymmetry abnormality in the *Smad5* mutants, but can be caused also by failure of ventral closure and/or deficiencies in the formation of lateral plate mesoderm.

Craniofacial abnormalities in Smad5 mutant embryos

Multiple BMP family member ligands and receptors are expressed in localized patterns during early embryonic development of the brain and within the neural crest-derived premigratory and postmigratory zones (Mehler et al., 1997; Dewulf et al., 1995). There is evidence that BMPs play a role in neurogenesis (Furuta et al., 1997) and neural tube closure by inducing apoptosis in the neuroectoderm (Mehler et al., 1997). Cephalic neural tube closure occurs normally when 15 to 18 pairs of somites have developed (Kaufman, 1992), but is

delayed or absent in several Smad5-deficient embryos (Figs 2O, 4K, 4M). Open neural tubes were also observed in a number of *BMP-2* mutants but were interpreted as secondary consequences of heart defects (Zhang and Bradley, 1996). Similarly, the neural tube closure defects in the *Smad5* knockout embryos is likely to be secondary to hemodynamic insufficiency resulting from severe yolk sac and heart lesions since apoptosis in the neuroectoderm (data not shown) and marker analysis for neural crest cells (*AP-2*, *twist*) (data not shown) were not significantly different between mutants and controls. These expression data demonstrate that neural crest cell differentiation, migration and subsequent population of the branchial arches is not influenced by the absence of Smad5 (data not shown).

DISCUSSION

We have shown that *Smad5* is expressed in a near ubiquitous pattern from gastrulation onwards. Despite its early postimplantation expression pattern, *smad5*[m1]/*smad5*[m1] embryos proceed beyond the egg cylinder stage, undergo gastrulation and initiate organogenesis. This raises the possibility that loss of the *Smad5* gene is compensated by other Smads with high sequence similarity and in vitro function to *Smad5* (e.g., *Smad1* and *Smad8*). Compensation of function could also explain why mutant mice lacking candidate ligands upstream of Smad5 (e.g., *BMP-2* and *BMP-4* knockout mice) (Zhang and Bradley, 1996; Winnier et al., 1995) or receptors (*ALK-3* knockouts; Mishina et al., 1995) display earlier and/or more severe features than our *Smad5* knockout mice and would also explain the low penetrance of some defects in the *Smad5* mutants. For example, *BMP-4* knockout mice generally fail to develop beyond the egg cylinder stage and ALK-3-deficient mice are embryonic lethal at E7.5-E9.5 due to lack of mesoderm formation. However, these 'compensatory' Smad(s) cannot fully rescue the defects in Smad5-deficient embryos since they eventually die at E9.5-E11.5. The reasons for this lack of total compensation may be that the expression pattern of *Smad5* and other Smads do not co-localize completely, that the presence of mRNA does not necessarily predict the presence of protein, or that the receptor-regulated Smads display a different subset of activities in ligand-activated cells.

Role of Smad5 in vascular development

A remarkable finding of our studies is that ectopic hematopoiesis and vasculogenesis occur in the amnion of *Smad5* mutant embryos. These sites first appear as aggregates of cells attached to the amnion next to the headfold, heart primordium or allantois at E8.0-E8.5. Histologically, these aggregates seem similar to allantois tissue. Molecular marker analysis (*AP-2*, *twist*, *Tbx2, flk-1* and *ζ-globin*) indicated that these cells are extraembryonic mesodermal cells with hematopoietic and vasculogenesis potential, which are also features of the allantois. Although both the extraembryonic mesoderm component of yolk sac allantois and amnion have blood-forming potential, under normal conditions, vasculogenesis only occur in the yolk sac and allantois but never in the amnion. Thus it has been hypothesized that vasculogenesis in the extraembryonic mesoderm is activated by

Fig. 4. Extraembryonic and embryonic vasculogenesis and hematopoiesis defects observed in $smad5^{m1}/smad5^{m1}$ embryos. (A) The yolk sac of a *Smad5* mutant was cleared in glycerol to reveal the amnion and allantois. In situ hybridization for (B) *AP-2* and (C) *twist* on transverse sections of an E8.5 *Smad5* mutant demonstrates that the *AP-2*-positive ectodermal component of the amnion does not undergo hyperplasia, and that the aggregate of cells is of extraembryonic mesodermal origin (C). (D) Whole-mount in situ hybridization for *Tbx-2* on E8.5 wild-type (left) and *Smad5* mutant (right) littermate. (E) Histology of the hemorrhagic structure in the amnion in the section at the level a in Fig. 2F. (F) *Flk-1* and (G) ζ-*globin* in situ hybridization demonstrate, respectively, ectopic vasculogenesis and hematopoiesis in the amnion of an E8.5 *Smad5* mutant. Yolk sac histology of (H) control and (I) *Smad5* mutant E9.5 littermates. (J,K) *Flk-1* and (L,M) ζ-*globin* in situ hybridization of wild-type and *Smad5* mutant. (F,G,K,M) Enlarged dorsal aorta are observed in mutant. (J,L) The control embryo almost completed turning, whereas (K,M) the mutant littermate did not initiate turning. Abbreviations: ag, aggregate of cells; al, allantois; am, amnion; bc, primitive blood cell; bw, body wall; da, dorsal aorta; ee, extraembryonic endoderm; em, endothelial and mesothelial layers; fg, foregut; he, heart; hg, hindgut; se, surface ectoderm; ve, blood vessel; ys, yolk sac. Scale bar: (A,D,F,G,J-M) 200 μm; (B,C,E) 100 μm; (H,I) 50 μm.
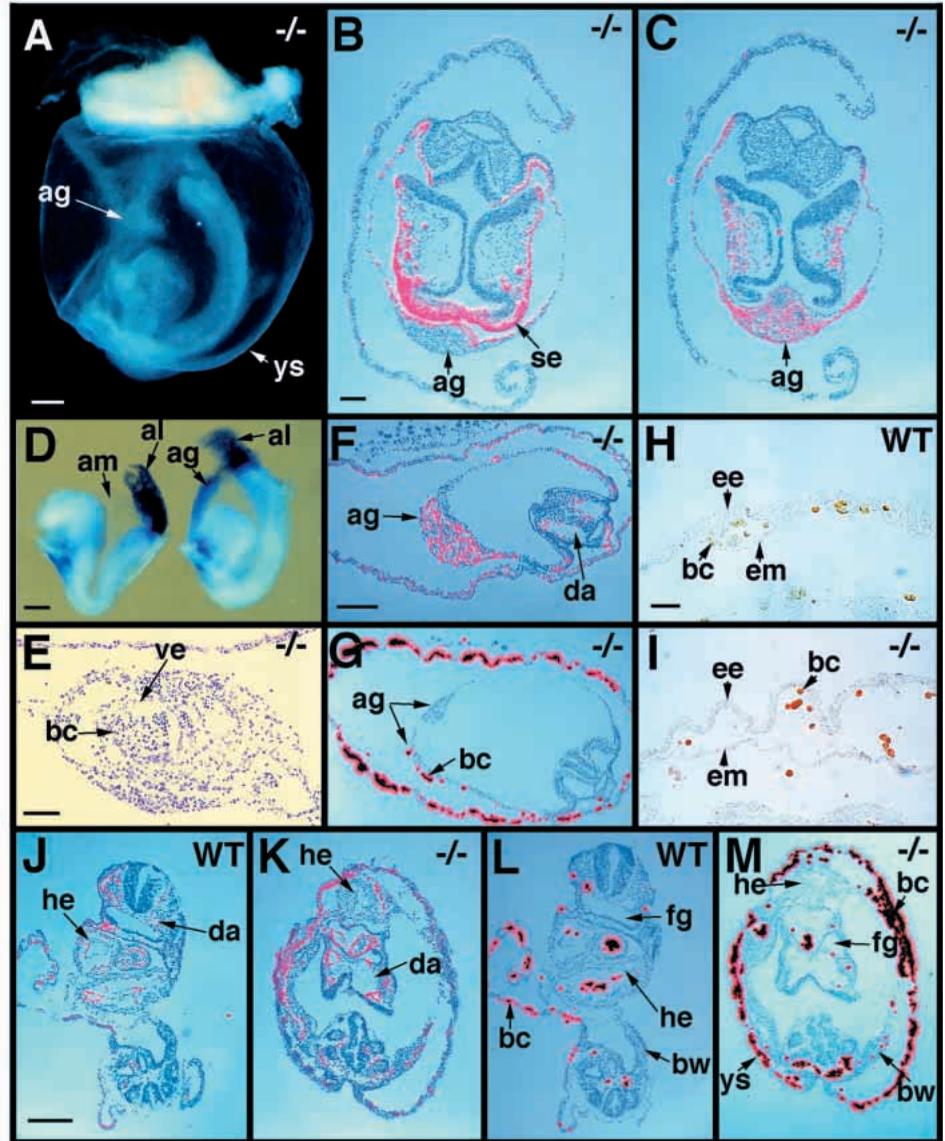
signals from the extraembryonic endodermal component of the yolk sac (Palis et al., 1995) and is inhibited by signals from the embryonic ectodermal component of the amnion (reviewed by Risau and Flamme, 1995). Little is known about the factors involved in the negative regulation of hematopoietic mesoderm differentiation. Ectopic vasculogenesis and hematopoiesis in *Smad5* mutant mice may suggest that Smad5 is participating in the inhibition of hematopoietic mesoderm differentiation. However, more likely as shown by *Tbx2* marker analysis, absence of Smad5 may have altered the cell sorting mechanism or migration resulting in mislocation of allantois tissue. Smad5 may also be involved in the negative regulation of hematopoietic cell proliferation in the yolk sac as suggested by the increased ζ-globin expression in the yolk sac of the majority of the mutant embryos.

Although the initial specification of both embryonic and extraembryonic endothelial cells is relatively intact in the absence of Smad5, as demonstrated by *flk-1* in situ hybridization, subsequent organization and integrity of the vessels are dependent on Smad5. Different mechanisms may underlie this vasculogenesis problem. The phenotype could originate from impaired ECM deposition, VEGF synthesis or signaling, or recruitment of pericytes and smooth muscle cells to participate in organization of the vessel wall.

Smad5, a putative component in TGF-β and ALK-1 signaling pathways

The impaired organization and maintenance of vessels in the absence of Smad5 is a phenotype superficially reminiscent of the mildest *BMP-4* knockout embryos (Winnier et al., 1995). However, the yolk sac lesions in the *BMP-4* knockout mice were attributed to the paucity of extraembryonic mesoderm and blood islands underlying the extraembryonic endodermal layer, which was already obvious at E8.5. Although Smad5 was not considered to be involved in TGF-β pathways in vitro (Attisano and Wrana, 1998), antisense technology in human hematopoietic lineages pointed to the involvement of Smad5 in intracellular signaling of *TGF-β1* (Bruno et al., 1998). In addition, the resemblance of the *Smad5* mutant yolk sac phenotype to the *TGF-β1* and *TβRII* knockouts as well as to

Fig. 5. Defective gut development in *smad5*[m1]/*smad5*[m1] embryos. Expression of *HNF3β* in (A,C,E) control and (B,D,F) mutant littermates as detected by in situ hybridization. Sagittal sections through (A,B) E7.5 and (E,F) E9.5 and (C,D) transverse sections through E8.5 embryos. Abbreviations: aaf, anterior amniotic fold; am, amnion; ec, ectoderm; en, endoderm; fb, forebrain; fd, future entrance of foregut diverticulum; fp, floorplate of neural tube; fg, foregut; fgd, entrance of foregut diverticulum; g, gut; hb, hindbrain; he, heart; hg, hindgut; hgd, entrance of hindgut diverticulum; m, mesoderm; nc, notochord; no, node; nt, neural tube; paf, posterior amniotic fold; ys, yolk sac. Scale bar: (A-D) 100 μm; (E,F) 200 μm.
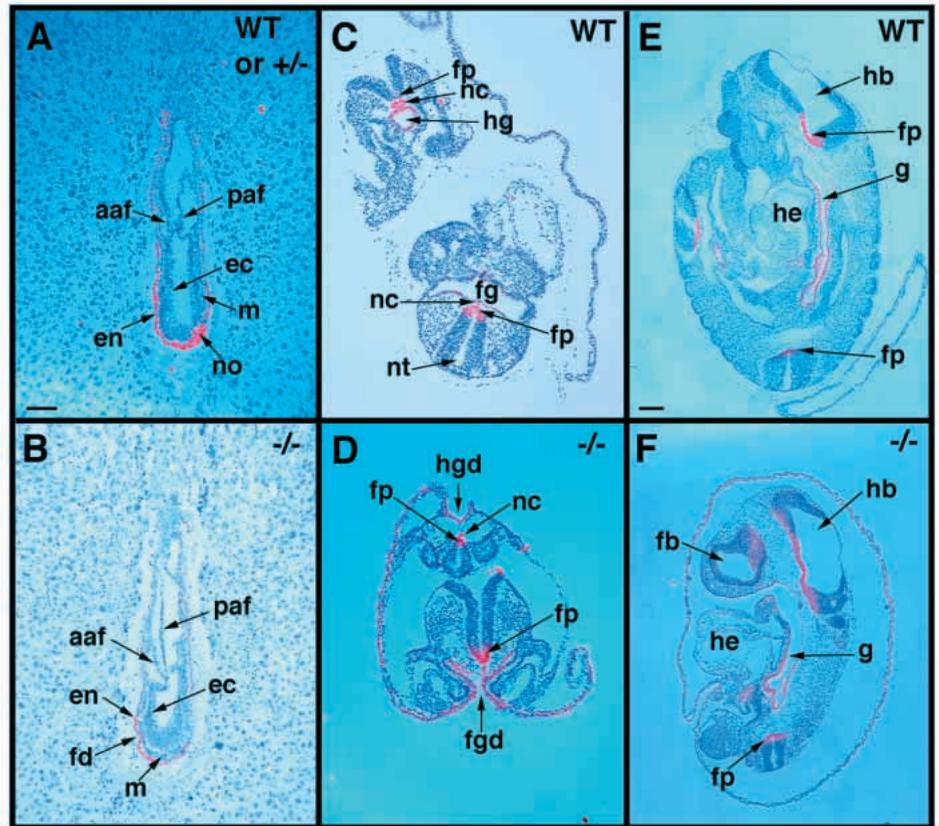

Fig. 6. Cardiac defects in *smad5*[m1]/*smad5*[m1] mutant embryos. *Nkx2.5* expression in the heart of (A) control and (B,C) *smad5*[m1]/*smad5*[m1] siblings, analyzed by whole-mount in situ hybridization. The embryos in A, B and C have developed 10, 11 and 11 pairs of somites, respectively. (D,E) Transverse sections through control and mutant E9.5 littermates. (E) A section at the level b indicated in Fig. 2F, showing the heart is exteriorized in the mutant. *GATA-4* expression in (F) control and (G) *smad5*[m1]/*smad5*[m1] E8.5 littermates, analyzed by in situ hybridization. A frontal and sagittofrontal section is shown respectively. Abbreviations: fg, foregut; fge, foregut entrance; mc, myocardium; ne, neuroectoderm; he, heart; ys, yolk sac. Scale bar: (A-C) 100 μm; (D, E) 200 μm; (F,G) 50 μm.
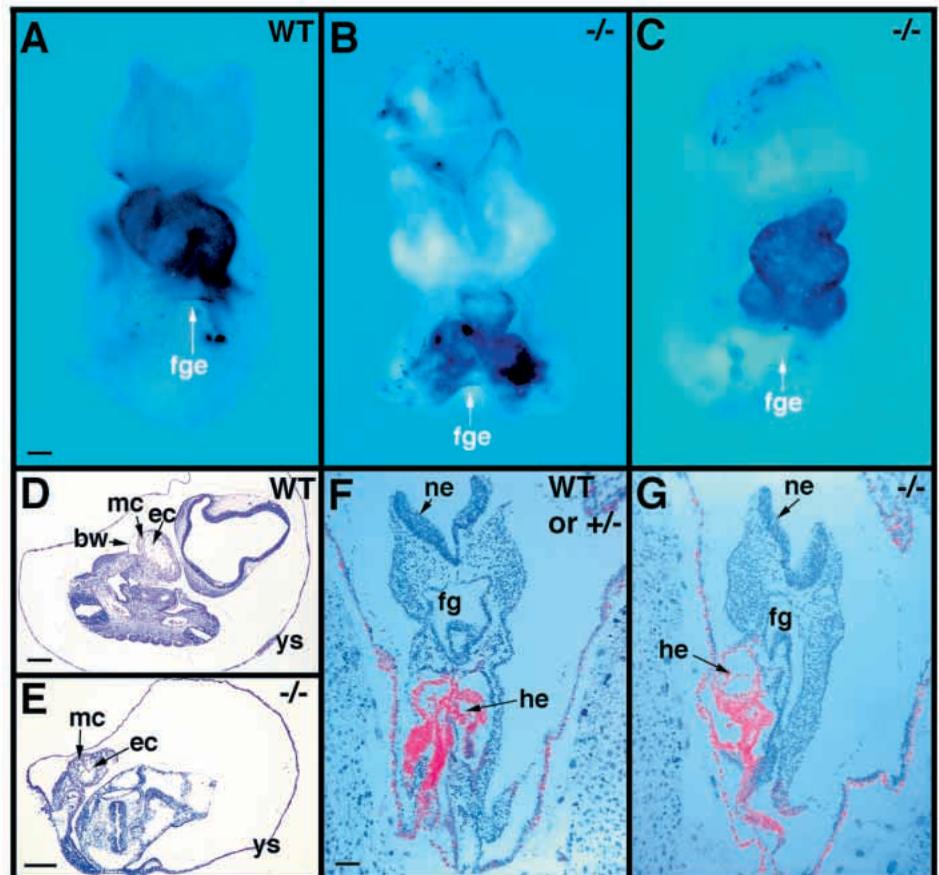
chimeras overexpressing a dominant negative truncated TβRII in the extraembryonic mesoderm of the yolk sac with regard to the failure of differentiating endothelial cells to assemble into robust vessels and reduced cellular adhesiveness of the yolk sac layers is striking (Dickson et al., 1995; Oshima et al., 1996; M. Goumans, A. Z., M. van Rooijen, D. H., B. Roelen and C. Mummery, unpublished data), and suggests that Smad5 is also a downstream mediator of TGF-β1 in vivo.

It is also remarkable that the vessel integrity defects in Smad5 mutant embryos and yolk sacs co-localize with cells and tissues expressing *ALK-1*, an orphan type I serine/threonine kinase receptor, for which TGF-β1 is a putative ligand (Roelen et al., 1997). *ALK-1* is predominantly expressed in extraembryonic mesoderm cells of the allantois and the yolk sac at E8.5. In the embryo proper, *ALK-1* is expressed in the dorsal aorta, sinus venosus, vitelline artery and, to a lesser extent, in the paraxial mesoderm and the cephalic mesenchyme. The vascular expression of *ALK-1* is maintained at later stages of development (Roelen et al., 1997). Thus, ALK-1 may play an important role in vasculogenesis, angiogenesis and maintenance of the vasculature (Roelen et al., 1997), which is further supported by linkage of autosomal dominant human disorders – hereditary hemorrhagic telangiectasia – to mutations in the *ALK-1* gene and endoglin, a membrane glycoprotein involved in binding and presenting TGF-β to its signaling receptors (Johnson et al., 1996, McAllister et al., 1994; Gallione et al., 1998). Therefore, it is tempting to speculate that Smad5 is not only a signal mediator downstream of activated ALK-3 and ALK-6, but also of ALK-1 similar to Smad1 (Macias-Silva et al., 1998). Functional studies in *Smad5* knockout cell lines and embryos will have to be performed in the future to test this hypothesis. It remains to be addressed if TGF-β and/or BMPs are both activators of ALK-1 and/or Smad5 in endothelial cells.

Smad5 in gut and cardiac development

The earliest discernible defect in some of the Smad5-deficient embryos was a vestigial foregut at the late headfold-early somite stage. Our findings suggest a role of BMP ligands and receptors in the developing foregut pocket, which is supported by their expression patterns. *ALK-3* is expressed ubiquitously from the advanced egg cylinder stage onwards (Dewulf et al., 1995), *BMP-4* is expressed in the foregut (Winnier et al., 1995) and *BMP-7* in the anterior foregut (Furuta et al., 1997), although there is no data available on their expression in progenitors of the definitive endoderm. Deficiency in Smad5 did not appear to affect definitive endoderm differentiation, as shown by the *HNF3β* in situ hybridization and, therefore, we speculate that Smad5 is required for the mechanical invagination of the definitive endoderm by the ventrolateral movement of the yolk sac and lateral plate mesoderm. Ventrolateral morphogenesis defects might be caused by proliferation or migration defects. Alternatively, the fate of the anterior visceral endoderm (AVE), rather than the definitive endoderm, might be altered and cause the gut and cardiac phenotype in *Smad5* mutants. *Otx-2* and *GATA-4* knockout embryos develop serious gut, cardiac and forebrain abnormalities, of which *Smad5* mutant phenotypes are superficially reminiscent. *GATA-4* knockout phenotypes are rescued in chimeric experiments, in which the embryo proper is derived of knockout ES cells and only the primitive and extraembryonic endoderm lineages are of wild-type origin (Narita et al., 1997; Rhinn et al., 1998). AVE derivatives (*lacZ* and *Otx-2* or *GATA-4* positive) can be traced in the rescued, phenotypical normal gut. These studies demonstrated that the prolonged presence of descendants of the AVE in the foregut plays a critical role in foregut development and anterior patterning as well as heart and forebrain development (Beddington and Robertson, 1998).

In some severely affected *Smad5* mutants, the hearts were localized in the exocoelomic cavity at E8.5 and E9.5. One possibility is that the above-mentioned gut and ventrolateral morphogenesis defects lead to the inappropriate localization of the heart primordium. BMP-2-deficient mice have to some extent a comparable phenotype in that the hearts are malpositioned. A similar, although more pronounced, exteriorization of the heart is also observed in *GATA-4* and *furin* knockout embryos (Kuo et al., 1997; Molkentin et al., 1998; Roebroeck et al., 1998). *Furin* is a convertase that processes precursor forms of TGF-β-related proteins. In addition, the cardiac primordia of GATA-4- and furin-deficient embryos do not fuse and they fail to form a normal foregut. In the case of the *BMP-2* knockouts, the heart was located in the exocoelomic cavity due to a lack of closure of the proamniotic canal (Zhang and Bradley, 1996), a defect never observed in our mutants. At later points, organization and fusion of the heart primordia, subsequent morphogenesis, and looping are clearly dependent on Smad5 function. It is unlikely that the defects in cardiac morphogenesis in Smad5-deficient embryos reflect a generalized developmental delay because these embryos formed structures such as dorsal aortas, multiple somites and limb buds, which normally develop subsequent to heart tube formation and initiation of looping. However, no misexpression of the BMP-2-inducible and cardiac-specific genes *Nkx2.5* and *GATA-4* was observed. This suggests that primary specification of the progenitors of the cardiac lineages was not affected and that signaling through Smad5 is not essential for either the initiation or maintenance of the normal expression of these genes.

CONCLUSION

In contrast to Smad2 and Smad4 (Nomura and Li, 1998; Waldrip et al., 1998; Weinstein et al., 1998; Sirard et al., 1998; Yang et al., 1998), Smad5 is not required for the initial formation of the embryonic and extraembryonic tissues at early postimplantation stages of mouse development. However, the role of Smad5 later in embryogenesis is complex and probably partially masked in our knockout study by functional compensation of related Smads. In the future, approaches such as tissue-specific gene targeting will be used to investigate more directly the role of Smad5 in specific organ development (e.g., the heart). Smad5 clearly plays a critical role in at least three developmental programs within the embryo. First, normal ventrolateral morphogenesis is shown here to require Smad5 function for proper gut and heart development. Secondly, Smad5 is essential to maintain the integrity of yolk sac and embryonic vasculature. Thirdly, Smad5 seems pivotal for normal amnion-allantois generation. Although some of the *Smad5* knockout phenotypes are reminiscent of knockouts of the Smad5-activating ligands, BMP-2 and BMP-4, the

vasculogenesis and hematopoiesis defects are indicative of Smad5 promiscuity towards pathways of other TGF-β members. We hypothesize that TGF-β1, ALK-1 and Smad5 are components of pathways that maintain vessel integrity and homeostasis in the visceral yolk sac and the embryo proper.

REFERENCES

Albrecht, U., Eichele, G., Helms, J. A. and Lu, H-C. (1997). Visualization of gene expression patterns by in situ hybridization. In *Molecular and Cellular Methods in Developmental Toxicology* (ed. G. P. Daston,) pp. 23-48. Boca Raton: CRC Press, Inc.

Andree, B., Duprez, D., Vorbusch, B., Arnold, H. H. and Brand, T. (1998). BMP-2 induces ectopic expression of cardiac lineage markers and interferes with somite formation in chicken embryos. *Mech. Dev.* **70,** 119-131.

Ang, S. L., Wierda, A., Wong, D., Stevens, K. A., Cascio, S., Rossant, J. and Zaret, K. S. (1993). The formation and maintenance of the definitive endoderm lineage in the mouse: involvement of HNF3/forkhead proteins. *Development* **119,** 1301-1315.

Ang, S. L. and Rossant, J. (1994). HNF-3β is essential for node and notochord formation in mouse development. *Cell* **78,** 561-574.

Attisano, L. and Wrana, J. L. (1998). Mads and Smads in TGFβ signalling. *Curr. Opin. Cell. Biol.* **10,** 188-194.

Beddington, R. S., Rashbass, P. and Wilson, V. (1992). Brachyury, a gene affecting mouse gastrulation and early organogenesis. *Development* **1992 Supplement**, 157-165.

Beddington R. S. and Robertson E. J. (1998). Anterior patterning in mouse. *Trends Genet.* **14,** 277-284.

Bradley, A. (1987). Production and analysis of chimaeric mice. Teratocarcinomas and embryonic stem cells: a practical approach. In *Production and Analysis of Chimaeric Mice.* (ed. E. J. Robinson). pp. 113-151. Oxford: IRL.

Bruno, E., Horrigan, S. K., Van Den Berg, D., Rozler, E., Fitting, P. R., Moss, S. T., Westbrook, C. and Hoffman, R. (1998). The Smad5 gene is involved in the intracellular signaling pathways that mediate the inhibitory effects of transforming growth factor-beta on human hematopoiesis. *Blood* **91,** 1917-1923.

Chen, Z. F. and Behringer, R. R. (1995). Twist is required in head mesenchyme for cranial neural tube morphogenesis. *Genes Dev.* **9,** 686-699.

Conlon, F. L., Lyons, K. M., Takaesu, N., Barth, K. S., Kispert, A., Herrmann, B. and Robertson, E. J. (1994) A primary requirement for nodal in the formation and maintenance of the primitive streak in the mouse. *Development* **120,** 1919-1928.

Dewulf, N., Verschueren, K., Lonnoy, O., Moren, A., Grimsby, S., Vande Spiegle, K., Miyazono, K., Huylebroeck, D. and ten Dijke, P. (1995). Distinct spatial and temporal expression patterns of two type I receptors for bone morphogenetic proteins during mouse embryogenesis. *Endocrinology* **136,** 2652-2663.

Dickson, M. C., Martin, J. S., Cousins, F. M., Kulkarni, A. B., Karlsson, S. and Akhurst, R. J. (1995). Defective haematopoiesis and vasculogenesis in transforming growth factor-beta 1 knockout mice. *Development* **121,** 1845-1854.

Furuta, Y., Piston, D. W. and Hogan, B. L. M. (1997). Bone morphogenetic proteins (BMPs) as regulators of dorsal forebrain development. *Development* **124,** 2203-2212.

Gallione, C. J., Klaus, D. J., Yeh, E. Y., Stenzel, T. T., Xue, Y., Anthony, K. B., McAllister, K. A., Baldwin, M. A., Berg, J. N., Lux, A., et al., (1998). Mutation and expression analysis of the endoglin gene in hereditary hemorrhagic telangiectasia reveals null alleles. *Hum. Mutat.* **11,** 286-294.

Goumans, M.-J., Ward-van Oostwaard, D., Wianny, F., Savatier, P., Zwijsen, A. and Mummery, C. (1998). Mouse embryonic stem cells with aberrant transforming growth factor beta signalling exhibit impaired differentiation in vitro and in vivo. *Differentiation* **63,** 101-113.

Heikinheino, M., Scandrett, J. M. and Wilson, D. B. (1994). Localization of transcription factor *GATA-4* to regions of the mouse embryo involved in cardiac development. *Dev. Biol.* **164,** 361-373.

Heldin, C. H., Miyazono, K. and ten Dijke, P. (1997). TGF-β signalling from cell membrane to nucleus through SMAD proteins. *Nature* **390,** 465-471.

Johnson, D. W., Berg, J. N., Baldwin, M. A., Gallione, C. J., Marondel, I., Yoon, S. J., Stenzel, T. T., Speer, M., Pericak-Vance, M. A., Diamond, A. et al., (1996). Mutations in the activin receptor-like kinase 1 gene in hereditary haemorrhagic telangiectasia type 2. *Nat. Genet.* **13,** 189-195.

Kaufman, M. H. (1992). *The Atlas of Mouse Development.* (ed. Kaufman, M. H.). London: Academic Press.

Kuo, C. T., Morrisey, E. E., Anandappa, R., Sigrist, K., Lu, M. M., Parmacek, M. S., Soudais, C. and Leiden, J. M. (1997). GATA4 transcription factor is required for ventral morphogenesis and heart tube formation. *Genes Dev.* **11,** 1048-1060.

Lau, A. L., Shou, W., Guo, Q. and Matzuk, M. M. (1997). Transgenic approaches to study the functions of the transforming growth factor-β superfamily members. In *Serono Symposia USA* (ed. T. Aono, H. Sugino and W. W. Vale). pp. 220-243. New York: Springer-Verlag, Inc.

Lawson, K. A. and Pedersen, R. A. (1987). Cell fate, morphogenetic movement and population kinetics of embryonic endoderm at the time of germ layer formation in the mouse. *Development* **101,** 627-652.

Leder, A., Kuo, A., Shen, M. M. and Leder, P. (1992). In situ hybridization reveals co-expression of embryonic and adult alpha globin genes in the earliest murine erythrocyte progenitors. *Development* **116,** 1041-1049.

Lints, T. J., Parsons, L. M., Hartley, L., Lyons, I. and Harvey, R. P. (1993). Nkx2. 5: a novel murine homeobox gene expressed in early heart progenitor cells and their myogenic descendants. *Development* **119,** 419-431.

Macias-Silva, M., Hoodless, P. A., Tang, S. J., Buchwald, M. and Wrana, J. L. (1998). Specific activation of smad1 signaling pathways by the BMP7 type I receptor, ALK2. *J. Biol. Chem.* **273,** 25628-25636.

Massagué, J. and Weis-Garcia, F. (1996). Serine/threonine kinase receptors: mediators of transforming growth factor beta family signals. *Cancer Surv.* **27,** 4 1-64.

Matzuk, M. M., Finegold, M. J., Su, J. G., Hsueh, A. J. and Bradley, A. (1992). Alpha-inhibin is a tumour-suppressor gene with gonadal specificity in mice. *Nature* **360,** 313-319.

McAllister, K. A., Grogg, K. M., Johnson, D. W., Gallione, C. J., Baldwin, M. A., Jackson, C. E., Helmbold, E. A., Markel, D. S., McKinnon, W. C., Murrell, J. et al., (1994). Endoglin, a TGF-beta binding protein of endothelial cells, is the gene for hereditary haemorrhagic telangiectasia type 1. *Nat. Genet.* **8,** 345-351.

Meersseman, G., Verschueren, K., Nelles, L., Blumenstock, C., Kraft, H., Wuytens, G., Remacle, J., Kozak, C. A., Tylzanowski, P., Niehrs, C. et al. (1997). The C-terminal domain of Mad-like signal transducers is sufficient for biological activity in the Xenopus embryo and transcriptional activation. *Mech. Dev.* **61,** 127-140.

Mehler, M. F., Mabie, P. C., Zhang, D. and Kessler, J. A. (1997). Bone morphogenetic proteins in the nervous system. *Trends Neurosci.* **20,** 309-317.

Millauer, B., Wizigmann-Voos, S., Schnurch, H., Martiniz, R., Mollen, P. H., Risau, W. and Ullrich, A. (1993). High affinity VEGF binding and developmental expression suggest *flk-1* as a major regulator of vasculogenesis and angiogenesis. *Cell* **72,** 835-846.

Mishina, Y., Suzuki, A., Ueno, N. and Behringer, R. R. (1995). Bmpr encodes a type I bone morphogenetic protein receptor that is essential for gastrulation during mouse embryogenesis. *Genes Dev.* **9,** 3027-3037.

Mitchell, P. J., Timmons, P. M., Hebert, J. M., Rigby, P. W. and Tijan, R. (1991). Transcription factor *AP-2* is expressed in neural crest cell lineages during mouse embryogenesis. *Genes Dev.* **5,** 105-119.

Molkentin, J. D., Lin, Q., Duncan, S. A. and Olson, E. N. (1997). Requirement of the transcription factor GATA4 for heart tube formation and ventral morphogenesis. *Genes Dev.* **11,** 1061-1072.

Narita, N., Bielinska, M., and Wilson, D. B. (1997). Cardiomyocyte

differentiation by *GATA-4*-deficient embryonic stem cells. *Development* **124,** 3755-3764.

Nishimura, R., Kato, Y., Chen, D., Harris, S. E., Mundy, G. R. and Yoneda, T. (1998). Smad5 and DPC4 are key molecules in mediating BMP-2-induced osteoblastic differentiation of the pluripotent mesenchymal precursor cell line C2C12. *J. Biol. Chem.* **273,** 1872-1879.

Nomura, M. and Li, E. (1998). Smad2 role in mesoderm formation, left-right patterning and craniofacial development. *Nature* **393,** 789-790.

Oshima, M., Oshima, H. and Takeo, M. M. (1996). TGF-β receptor type II deficiency results in defects of yolk sac hematopoiesis and vasculogenesis. *Dev. Biol.* **179,** 297-302.

Papaioannou, V. E. (1997). T-box family reunion. *Trends Genet.* **13,** 212-213.

Palis, J., McGrath, K. E. and Kingsley, P. D. (1995). Initiation of hematopoiesis and vasculogenesis in murine yolk sac explants. *Blood* **86,** 156-163.

Rhinn, M., Dierich, A., Shawlot, W., Behringer, R. R., Le Meur, M. and Ang, S. L. (1998). Sequential roles for Otx2 in visceral endoderm and neuroectoderm for forebrain and midbrain induction and specification. *Development* **125,** 845-856.

Risau, W. and Flamme, I. (1995). Vasculogenesis. *Annu. Rev. Cell Dev. Biol.* **11,** 73-91.

Roebroek, A. J. M., Umans, L., Paull, I. G. L., Robertson, E. J., van Leuven, F., van de Ven, W. J. M. and Constam, D. B. (1998). Failure of ventral closure and axial rotation in embryos lacking the proprotein convertase Furin. *Development* **125,** 4863-4876.

Roelen, B. A. J., van Rooijen M. A. and Mummery, C. L. (1997). Expression of ALK-1, a type 1 serine/threonine kinase receptor, coincides with sites of vasculogenesis and angiogenesis in early mouse development. *Dev. Dyn.* **209,** 418-430.

Schott, J. J., Benson, D. W., Basson, C. T., Pease, W., Silberbach, G. M., Moak, J. P., Maron, B. J., Seidman, C. E., Seidman, J. G. (1998). Congenital heart disease caused by mutations in the transcription factor *Nkx*2-5. *Science* **281,** 108-111.

Sirard, C., de la Pompa, J. L., Elia, A., Itie, A., Mirtsos, C., Cheung, A., Hahn, S., Wakeham, A., Schwartz, L., Kern, S. E. et al., (1998). The tumor suppressor gene Smad4/Dpc4 is required for gastrulation and later for anterior development of the mouse embryo. *Genes Dev.* **12,** 107-119.

Stoetzel, C., Weber, B., Bourgeois, P., Bolcato-Bellemin, A. L. and Phmitt Ferrin, S. C. (1995). Dorso-ventral and rostro-caudal sequential expression of M-twist in the postimplantation murine embryo. *Mech. Dev.* **51,** 251-263.

Suzuki, A., Chang, C., Yingling, J. M., Wang, X. F. and Hemmati-Brivanlou, A. (1997). Smad5 induces ventral fates in Xenopus embryo. *Dev. Biol.* **184,** 402-405.

Tam, P. P. L. and Beddington, R. S. P. (1992). Establishment and organisation of germlayers in the gastrulating mouse embryo. *CIBA Found. Symp.* **165,** 27-49.

Tamaki, K., Souchelnytskyi, S., Itoh, S., Nakao, A., Sampath, K., Heldin, C. H., ten Dijke, P. (1998). Intracellular signaling of osteogenic protein-1 through Smad5 activation. *J. Cell Physiol.* **177,** 355-363.

Waldrip, W. R., Bikoff, E. K., Hoodless, P. A., Wrana, J. L. and Robertson, E. J. (1998). Smad2 signaling in extraembryonic tissues determines anterior-posterior polarity of the early mouse embryo. *Cell* **92,** 797-808.

Weinstein, M., Yang, X., Li, C., Xu, X., Gotay, J. and Deng, C. X. (1998). Failure of egg cylinder elongation and mesoderm induction in mouse embryos lacking the tumor suppressor smad2. *Proc. Natl. Acad. Sci. USA* **95,** 9378-9383.

Winnier, G., Blessing, M., Labosky, P. A. and Hogan, B. L. (1995). Bone morphogenetic protein-4 is required for mesoderm formation and patterning in the mouse. *Genes Dev.* **9,** 2105-2116.

Yamamoto, N., Akiyama, S., Katagiri, T., Namiki, M., Kurokawa, T. and Suda, T. (1997). Smad1 and *smad5* act downstream of intracellular signalings of BMP-2 that inhibits myogenic differentiation and induces osteoblast differentiation in C2C12 myoblasts. *Biochem. Biophys. Res. Commun.* **238,** 574-580.

Yang, X., Li, C., Xu, X. and Deng, C. (1998). The tumor suppressor SMAD4/DPC4 is essential for epiblast proliferation and mesoderm induction in mice. *Proc. Natl. Acad. Sci. USA* **95,** 3667-3672.

Zhang, H. and Bradley, A. (1996). Mice deficient for BMP2 are nonviable and have defects in amnion/chorion and cardiac development. *Development* **122,** 2977-2986.

Zhang, J., Hagopian-Donaldson, S., Serbedzija, G., Elsemore, J., Plehn-Dujowich, D., McMahon, A. P., Flavell, R. A. and Williams, T. (1996). Neural tube, skeletal and body wall defects in mice lacking transcription factor *AP-2*. *Nature* **381,** 238-241.

Zhu, Y., Richardson, J. A., Parada, L. F., Graff, J. M. (1998). Smad3 mutant mice develop metastatic colorectal cancer. *Cell* **96,** 703-714.

Zwijsen, A., Goumans, M. J., Lawson, K. A., van Rooijen, M. A. and Mummery, C. L. (1999). Ectopic expression of the transforming growth factor type II receptor disrupts mesoderm organisation during mouse gastrulation. *Dev. Dyn.*, In press.